

# Glass-Transition Temperatures in CO<sub>2</sub> + Polymer Systems: Modeling and Experiment

Anupama Kasturirangan,<sup>†</sup> Carolyn A. Koh,<sup>‡</sup> and Aryn S. Teja<sup>\*,†</sup>

School of Chemical & Biomolecular Engineering, Georgia Institute of Technology, Atlanta, Georgia 30332-0100, and Department of Chemical Engineering, Colorado School of Mines, Golden, Colorado 80401

We extend a previously published compressible lattice model to the prediction of glass-transition temperatures in CO<sub>2</sub> + polymer systems. We have applied the model to published data as well as to new measurements of glass-transition temperatures in CO<sub>2</sub> + poly(methyl methacrylate) (PMMA) and CO<sub>2</sub> + poly(lactic acid) (PLA) systems. We demonstrate that the model is able to predict glass-transition temperatures in CO<sub>2</sub> + polymer systems using a parameter that is obtained from sorption data and a second parameter that is obtained from FTIR measurements. The parameters are not dependent on temperature, pressure, or polymer molecular weight.

## 1. Introduction

The use of supercritical CO<sub>2</sub> as an environmentally benign solvent and/or reaction medium for processing polymers has been well-documented.<sup>1,2</sup> The ability of CO<sub>2</sub> to swell biocompatible polymers and reduce their glass-transition temperature ( $T_g$ ) values, thereby facilitating the diffusion of small drug molecules into such polymers, has also led to much interest in using CO<sub>2</sub> in drug delivery applications.<sup>3,4</sup> It has been suggested that (i) CO<sub>2</sub> acts as a Lewis acid in the presence of Brønsted and Lewis bases<sup>5–8</sup> and (ii) these interactions have a significant effect on phase equilibria and physical properties of CO<sub>2</sub> + polymer systems. This could be the reason why otherwise immiscible polymers can be made soluble<sup>9</sup> in CO<sub>2</sub> by incorporating carbonyl C=O groups that interact with CO<sub>2</sub> and why the solubility of CO<sub>2</sub> in polymers such as poly(methyl methacrylate) (PMMA) that contain C=O groups is greater than the solubility of CO<sub>2</sub> in polymers without such groups, such as polystyrene (PS) or poly(vinyl chloride) (PVC). These observations imply that the Lewis acid character of CO<sub>2</sub> leads to significant interactions between the C atom in CO<sub>2</sub> and the C=O oxygen atom.<sup>10</sup> Knowledge of these interactions must be incorporated in models to describe CO<sub>2</sub> + polymer thermodynamic properties. Recently, we have proposed a compressible lattice model that is able to correlate cloud points and sorption equilibria in such systems using two parameters that do not depend on temperature or molecular weight.<sup>11,12</sup> In addition, we have shown that it is possible to obtain one of the parameters from independent measurements (such as FTIR spectra) and therefore, low-pressure CO<sub>2</sub> sorption behavior in polymers can be predicted using a single parameter obtained from high-pressure cloud point data.<sup>12</sup>

In the present study, we extend the model to the prediction of glass-transition temperatures in CO<sub>2</sub> + polymer systems. We test the model using published data as well as new measurements for glass-transition temperatures in CO<sub>2</sub> + PMMA and CO<sub>2</sub> + poly(lactic acid) (PLA) systems. The ultimate goal of this work is to make *a priori* predictions of phase behavior, glass-transition

temperatures, and sorption behavior in CO<sub>2</sub> + polymer systems in which there are specific interactions between CO<sub>2</sub> and a functional group in the polymer segment.

## 2. Compressible Lattice Model

In this model, a CO<sub>2</sub> + polymer solution is assumed to consist of associated and unassociated polymer segments, as well as associated and unassociated CO<sub>2</sub> molecules arranged on a lattice. Specific interactions between CO<sub>2</sub> and a functional group in a polymer segment restrict a certain number of CO<sub>2</sub> molecules to specific lattice sites. On the other hand, unassociated CO<sub>2</sub> molecules are distributed randomly on the lattice. The total number of configurations of these molecules and segments leads to an entropy of mixing which, combined with an enthalpy of mixing based on contacts resulting from association and dispersion, results in the following expression for the Gibbs energy of mixing  $\Delta G^{\text{mix}}$ :

$$\frac{\Delta G^{\text{mix}}}{NRT} = \alpha\mu\phi_2\chi_a + \phi_2\{1 - \phi_2(1 + \alpha\mu)\}[(z - 2 - \mu)\alpha + (1 - \alpha)(z - 2)]\chi_u + \frac{\phi_2}{\xi} \ln \phi_2 + \left[ \frac{1 - \phi_2(1 + \mu\alpha)}{1 + \mu\alpha} \right] \times \ln[1 - \phi_2(1 + \mu\alpha)] - \phi_1 \ln \left( \frac{\phi_1}{\phi_1 - \mu\alpha\phi_2} \right) + \mu\alpha\phi_2 \ln \left( \frac{\mu\alpha\phi_2}{\phi_1 - \mu\alpha\phi_2} \right) + \phi_2(1 - \alpha) \ln(1 - \alpha) + \alpha\phi_2 \ln \alpha \quad (1)$$

In eq 1,  $z$  is the lattice coordination number (in this work, a value of  $z = 10$  is assumed),  $R$  the gas constant,  $T$  the temperature,  $\phi_1$  the volume fraction of CO<sub>2</sub>, and  $\phi_2$  the volume fraction of polymer. There are five characteristic quantities in eq 1, namely, the solvent–segment binding ratio ( $\mu$ ), the association ratio ( $\alpha$ ), the number of segments ( $\xi$ ), and the two interaction parameters for association ( $\chi_a$ ) and dispersion ( $\chi_u$ ). The association parameter  $\chi_a$  is related to the enthalpy of association  $\Delta H_a$  for the binding reaction, according to

$$\chi_a = \frac{\Delta H_a}{RT} \quad (2)$$

and is therefore related to the equilibrium constant  $K$  for the binding reaction via the van't Hoff relationship:

\* To whom correspondence should be addressed. Tel: 404-894-3098. Fax: 404-894-2866. E-mail: amyn.teja@chbe.gatech.edu.

<sup>†</sup> School of Chemical & Biomolecular Engineering, Georgia Institute of Technology.

<sup>‡</sup> Department of Chemical Engineering, Colorado School of Mines.

$$\ln\left(\frac{K}{K_0}\right) = \frac{-\Delta H_a}{R}\left(\frac{1}{T} - \frac{1}{T_0}\right) \quad (3)$$

where  $K_0$  is the equilibrium constant for association at a reference temperature  $T_0$  (in this work,  $T_0 = 280$  K). The equilibrium constant  $K$  (and, therefore,  $\chi_a$ ) is related to the association ratio  $\alpha$ , or the fraction of associated segments per molecule, according to

$$\alpha = \frac{(1 + K) - \sqrt{(1 + K)^2 - 4\phi_1\phi_2K(1 + K)}}{2\phi_2(1 + K)} \quad (4)$$

Therefore,  $\chi_a$  and  $\alpha$  may be replaced by  $\Delta H_a$  and  $K_0$  in the model. The binding ratio  $\mu$  represents the number of  $\text{CO}_2$  molecules that can associate with a functional group. It has a value of 1 when only one  $\text{CO}_2$  molecule is able to associate with a functional group in a polymer segment, as is the case for all systems investigated in the present study. The dispersion parameter  $\chi_u$  is a measure of dispersion interactions between  $\text{CO}_2$  and the polymer segment and can be estimated from the solubility parameters  $\delta_1$  of  $\text{CO}_2$  and  $\delta_2$  of the nonpolar analog (or homomorph) of the polymer, according to

$$\chi_u = \frac{V_1(\delta_1 - \delta_2)^2}{RT(z - \mu\alpha - 2)} \quad (5)$$

where the functional group in the polymer molecule that interacts with  $\text{CO}_2$  is substituted with a nonpolar group to obtain the homomorph. In eq 5,  $V_1$  is the molar volume of  $\text{CO}_2$  and the other quantities have been defined previously. The segment ratio is obtained from the molar and van der Waals volumes of  $\text{CO}_2$  and polymer, according to

$$\xi = \frac{V_2[T, P] - 1.2V_2^{\text{vdW}}}{V_1[T, P] - V_1^{\text{vdW}}} \quad (6)$$

The molar volume of  $\text{CO}_2$  ( $V_1$ ) can be calculated from an equation of state (such as that of Patel and Teja<sup>13</sup> used in our calculations), and the molar volume of the polymer ( $V_2$ ) can be calculated using the group contribution modified cell model (GCMCM) of Sato et al.<sup>14</sup> or another method.

We have shown<sup>12</sup> that the resulting model is capable of simultaneously correlating both cloud points and sorption behavior in  $\text{CO}_2$  + polymer systems using two parameters ( $\Delta H_a$  and  $K_0$ ). Furthermore, we have shown that  $\Delta H_a$  may be obtained from FTIR measurements on polymer films exposed to  $\text{CO}_2$ , so that only one adjustable parameter is required in the calculations. An example of our calculations is shown in Figures 1a and 1b, where experimental and calculated cloud points and sorption behavior in the  $\text{CO}_2$  + PLA system are plotted using a value of  $\Delta H_a = -3.6$  kJ mol<sup>-1</sup> from FTIR measurements<sup>12</sup> and a single value of  $K_0 = 1.16$  is used to fit both cloud point data and sorption data. Note that the data cover a range of pressures that span more than 100 MPa and that the cloud points were correlated for two PLA samples with average molecular weights of 84 500 and 128 450.

**2.1. Extension of the Model To Calculate the Glass-Transition Temperature ( $T_g$ ).** To obtain glass-transition temperatures, we have combined the above model with the Gibbs–DiMarzio criterion,<sup>15,16</sup> which states that the system is in one of its lowest permissible energy configurations (or its “ground state” of amorphous packing) at the glass transition. Therefore, the configurational entropy of the system may be assumed to be zero<sup>15,16</sup> and

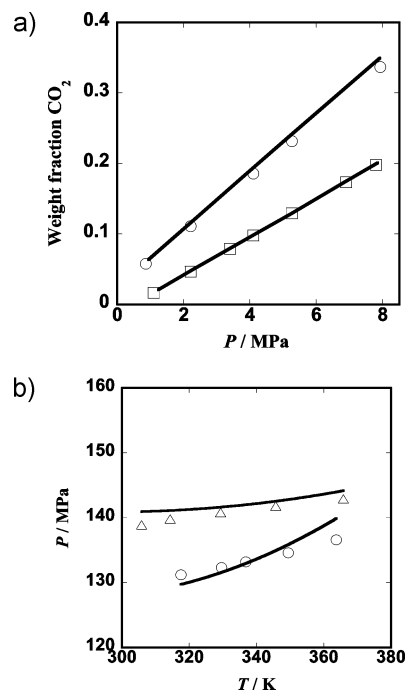


**Figure 1.** (a) Sorption of  $\text{CO}_2$  in PLA at (○) 313.15 K and (□) 344.15 K. Solid lines are predictions of the compressible lattice model with  $\Delta H_a = -3.6$  kJ mol<sup>-1</sup> and  $K_0 = 1.16$ . Data are taken from Kasturirangan et al.<sup>12</sup> (b) Cloud point behavior of  $\text{CO}_2$  + PLA, using experimental data from Conway et al.<sup>28</sup> for the polymers with molecular weights of (○)  $M_w = 84\,500$  and (△)  $M_w = 128\,450$ . Solid lines represent calculated values with  $\Delta H_a = -3.6$  kJ mol<sup>-1</sup>,  $K_0 = 1.16$ , and ~5.0 wt % polymer.

$$S_1 + S_2 + \Delta S^{\text{mix}} = 0 \quad (7)$$

where  $S_1$  is the configurational entropy of  $\text{CO}_2$  and  $S_2$  is the configurational entropy of the polymer at the glass-transition temperature. The configurational entropy of the polymer and of  $\text{CO}_2$  can be estimated from their equations of state, whereas the entropy of mixing ( $\Delta S^{\text{mix}}$ ) is obtained from the compressible lattice model. Since the concentration of  $\text{CO}_2$  in the polymer is also needed to calculate the terms in eq 7, the glass-transition temperature is obtained by simultaneously solving eq 7 and the thermodynamic criterion for sorption equilibrium between  $\text{CO}_2$  in the fluid and polymer phases. Thus,

$$\varphi_1(T, P)P = x_1\gamma_1^{\text{ol}}f_1^{\text{ol}} \quad (8)$$

In eq 8, the gas phase is assumed to be pure  $\text{CO}_2$  and its fugacity  $\varphi_1$  is obtained from an equation of state. The activity coefficient  $\gamma_1$  of  $\text{CO}_2$  in the polymer phase is obtained from the compressible lattice model and the fugacity of  $\text{CO}_2$  in its standard state  $f_1^{\text{ol}}$  from the Prausnitz–Shair correlation. Energies of interaction ( $\Delta H_a$ ) from FTIR measurements and  $K_0$  values required in the model were obtained by fitting cloud point or sorption data (depending on data availability). Equations 7 and 8 can be solved simultaneously for  $T_g$  and the corresponding  $\text{CO}_2$  concentration in the polymer at a fixed pressure. We have done this for systems for which sorption and  $T_g$  data were available (or measured in this work). The results are plotted in Figures 2–5 and discussed further in the following sections. Note that the plots cover a limited range of pressures, because sorption data were only available at these pressures for the systems that were studied.

### 3. Experimental Section

Since few data have been published for associated  $\text{CO}_2$  + polymer systems, differential scanning calorimetry (DSC) was

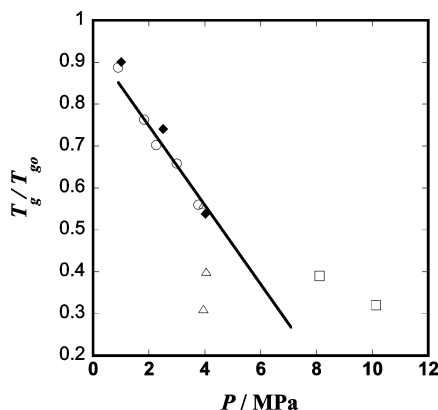


**Figure 2.** Glass-transition temperature ( $T_g$ ) values of the  $\text{CO}_2$  + PMMA system, as a function of  $\text{CO}_2$  pressure. Symbol legend: data of (○) Handa et al.,<sup>19</sup> (△) Wissinger and Paulaitis;<sup>17</sup> (□) Kikic et al.;<sup>20</sup> and (◆) this work. Solid line represents calculations using the compressible lattice model with  $\Delta H_a = -4.0 \text{ kJ mol}^{-1}$  and  $K_0 = 0.126$ .

used to measure the glass-transition temperatures in  $\text{CO}_2$  + PMMA and  $\text{CO}_2$  + PLA systems in the present study. These systems were chosen because they have been shown<sup>12</sup> to exhibit specific interactions between the C=O group and  $\text{CO}_2$ , and these interactions are expected to significantly affect  $T_g$ . The DSC technique provides rapid and accurate information on glass to rubbery transitions, provided that corrections are applied for increases in pressure during a scan and for baseline stability at elevated pressures. We employed a Setaram differential scanning calorimeter (Model  $\mu$ -DSCVIIa, Setaram, France) in our experiments. This DSC apparatus employs Peltier cooling to achieve temperatures as low as 230 K, and it can also achieve temperatures as high as 393 K. These temperatures can be held constant during an experiment, or a temperature scan can be initiated over a predetermined range. The DSC was coupled to high-pressure cells that are able to withstand pressures up to 40 MPa and hold  $0.5 \text{ cm}^3$  of material. A single-stage compression unit was used to compress  $\text{CO}_2$  to the desired pressure. Polymer samples were heated at rate of  $0.1 \text{ K min}^{-1}$  over a temperature range of 233–373 K through four heating and cooling cycles to eliminate any effects of thermal history and aging. The glass transition was identified from the change in heat flow resulting from a change in heat capacity at the transition temperature during each scan.

## 4. Results

**4.1.  $\text{CO}_2$  + Poly(methyl methacrylate) (PMMA).** Figure 2 presents our  $T_g$  measurements in the  $\text{CO}_2$  + PMMA system. (The data have been normalized with  $T_{g0}$ , which represents the glass-transition temperature of the polymer in the absence of  $\text{CO}_2$ .) The results show that  $T_g$  decreases monotonically as the pressure increases up to  $\sim 4 \text{ MPa}$ . Also plotted are the  $T_g$  measurements of Wissinger and Paulaitis<sup>17,18</sup> from creep compliance experiments, as well as the high-pressure DSC measurements of Handa et al.<sup>19</sup> and the chromatographic measurements of Kikic et al.<sup>20</sup> The four sets of measurements generally agree with each other, within their experimental uncertainties, up to pressures of  $\sim 4 \text{ MPa}$ . At higher pressures, however, the Wissinger and Paulaitis<sup>17</sup> data and the Handa et al.<sup>19</sup> data follow rather different trends. Wissinger and Paulaitis reported that the polymer adopts a liquid state beyond a maximum pressure at all temperatures above room temperature. Condo et al.<sup>21</sup> explained this behavior in terms of enhanced chain mobility resulting from the dissolution of  $\text{CO}_2$  into the polymer at low temperatures. The Sanchez–Lacombe equation

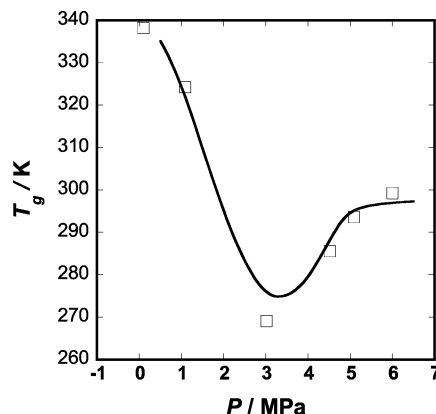


**Figure 3.** Glass-transition temperature ( $T_g$ ) values of the  $\text{CO}_2$  + PLA system. Square symbols (□) represent experimental data from this work, and the solid line represents the compressible lattice model predictions with  $\Delta H_a = -3.6 \text{ kJ mol}^{-1}$  and  $K_0 = 1.16$ .

and other EOSs with temperature-dependent binary interaction parameters have been used to correlate this type of retrograde vitrification.<sup>22,23</sup> However, the location of the pressure maximum in these calculations depends entirely on the magnitude of the binary interaction parameter used. In contrast, no pressure maximum is observed in the data of Kikic et al.,<sup>20</sup> and their  $T_g$  values continue to decrease monotonically as the pressure increases beyond 4 MPa. Our model was used to predict  $T_g$  values in this system with  $\Delta H_a = -4 \text{ kJ mol}^{-1}$  (from FTIR measurements) and  $K_0 = 0.126$  (by fitting sorption data). No adjustable parameters were used to predict  $T_g$  values. As can be seen from Figure 2, our predicted values of  $T_g$  are in excellent agreement with the Handa data and in qualitative agreement with the Kikic data. The phenomenon of retrograde vitrification is not predicted by our model.

**4.2.  $\text{CO}_2$  + Poly(lactic acid) (PLA).** Our  $T_g$  measurements in this system are shown in Figure 3. The data indicate a minimum in  $T_g$  as the  $\text{CO}_2$  pressure increases and an eventual leveling out of the  $T_g$  depression. The initial addition of  $\text{CO}_2$  to the polymer results in an increase in the polymer free volume and a decrease in  $T_g$ . At higher pressures, the effect of hydrostatic  $\text{CO}_2$  pressure dominates and leads to an increase in  $T_g$ . Particularly interesting is the steep depression of  $\sim 60 \text{ K}$  between pressures of 0.1 MPa and 3 MPa in this system. This behavior, as well as the  $T_g$  versus  $P$  curve, is reproduced remarkably well by our model, without any adjustable parameters. Note that the same values of  $\Delta H_a = -3.6 \text{ kJ mol}^{-1}$  (from FTIR measurements) and  $K_0 = 1.16$  (by fitting sorption data) were used in the calculations of cloud points, sorption, and glass transitions in this system.

**4.3.  $\text{CO}_2$  + Poly(styrene) (PS).** Figure 4 shows the  $T_g$  vs  $P$  curve for the  $\text{CO}_2$  + PS system predicted by our model. Also shown are experimental data from Wissinger and Paulaitis<sup>17</sup> from creep compliance experiments, Zhang and Handa<sup>24</sup> from high-pressure DSC scans, and of Kikic et al.<sup>20</sup> from chromatographic experiments. Our model predictions are in fair agreement with the Wissinger and Paulaitis data, although deviations are seen at higher pressures. Note that the two parameters  $\Delta H_a$  and  $K_0$  were set to zero in these calculations, since there are no specific interactions in this system. However,  $\chi_u$  was obtained by fitting the sorption data<sup>25</sup> in this case. The absence of specific interactions in  $\text{CO}_2$  + PS explains the low plasticization effect by  $\text{CO}_2$ .

**4.4.  $\text{CO}_2$  + Poly(ethyl methacrylate) (PEMA).** Excellent agreement was seen between model predictions and the glass-transition data of Kamiya et al.<sup>26</sup> from dielectric relaxation

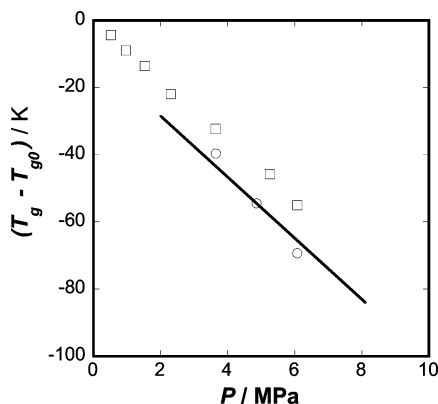


**Figure 4.** Glass-transition temperature ( $T_g$ ) values of the  $\text{CO}_2$  + PS system. Symbol legend: data of ( $\square$ ) Zhang et al.<sup>24</sup> and ( $\circ$ ) Wissinger;<sup>18</sup> the solid line represents model predictions using  $\Delta H_a = 0$  and  $K_0 = 0$ .

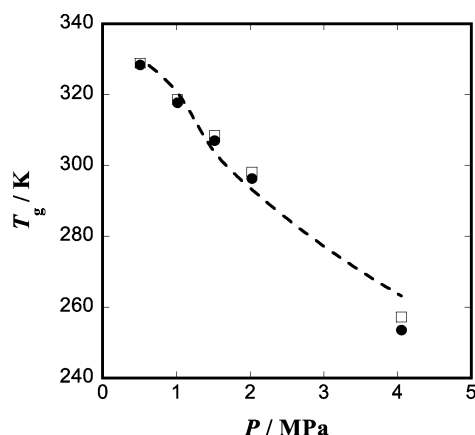


**Figure 5.** Glass-transition temperature ( $T_g$ ) values of the  $\text{CO}_2$  + PEMA system. Symbol legend: ( $\bullet$ ) data from Kamiya et al.<sup>26</sup> and ( $\square$ ) data from Condo et al.;<sup>27</sup> the dashed line represents model predictions using  $\Delta H_a = -3.9 \text{ kJ mol}^{-1}$  and  $K_0 = 0.17$ .

**Table 1.** Factors That Influence the Plasticization of Four Polymers by  $\text{CO}_2$

|                            | PS   | PMMA  | PEMA | PLA  |
|----------------------------|------|-------|------|------|
| $dT_g/dP$                  | 0.88 | 1.0   | 2.1  | 2.4  |
| $K_0$                      | 0    | 0.126 | 0.17 | 1.16 |
| $-\Delta H_a$ (kJ/mol)     | 0    | 4     | 3.9  | 3.6  |
| $V_f$ (cm <sup>3</sup> /g) | 0.95 | 0.82  | 0.88 | 0.69 |

measurements and Condo et al.<sup>27</sup> from creep compliance measurements. As seen in Figure 5, the addition of the  $\text{CH}_2$  group to the alkyl tail increases the polymer free volume and favors interaction with  $\text{CO}_2$ . Positive contributions from both the increase in free volume and specific interactions result in enhanced plasticization. As a consequence, both the sorption and  $T_g$  depressions are greater in PEMA than in PMMA.

## 5. Discussion

Three factors seem to be important in determining the  $T_g$  values in  $\text{CO}_2$  + polymer systems: specific interactions (as given by  $-\Delta H_a$ ), the number of complexes in solution (related to  $K_0$ ) and the free volume of the polymer. This is evident from values of the initial slope of the  $T_g$  vs  $P$  curve ( $dT_g/dP$ ) tabulated for four polymers (PS, PMMA, PEMA, PLA) in Table 1. Also tabulated are values of  $K_0$  and  $\Delta H_a$  and the polymer free volume calculated using the GCMCM model.<sup>14</sup> Note that PLA has the lowest polymer free volume among these polymers, but the largest  $dT_g/dP$  value, because it forms many complexes with

lactic acid segments (largest  $K_0$  value). Polystyrene, on the other hand, exhibits the lowest  $dT_g/dP$  value, despite having the largest free volume, because there are no specific interactions in this system.

## 6. Conclusions

The compressible lattice model has been employed successfully to correlate/predict phase equilibria in several  $\text{CO}_2$  + polymer systems. The parameters of this model have shown excellent extrapolative ability across polymer molecular weight, temperature, and pressure (high-pressure cloud-point curves and low-pressure sorption equilibria). The model was extended to the prediction of glass-transition temperature ( $T_g$ ) values in this work by application of the Gibbs–DiMarzio criterion. New data on  $T_g$  depressions in the  $\text{CO}_2$  + PMMA and  $\text{CO}_2$  + PLA systems were obtained using high-pressure differential scanning calorimetry. The  $\text{CO}_2$  + PMMA data generally agree with published data, although the phenomenon of retrograde vitrification was neither observed in our experiments nor predicted by our model.  $\text{CO}_2$  was observed to have a strong plasticization effect on PLA at all pressures, and the  $\text{CO}_2$  + PLA system was observed to exhibit a  $T_g$  minimum, because of opposing effects from plasticization and hydrostatic  $\text{CO}_2$  pressure. It proved possible to predict this minimum using our model in excellent agreement with experiment. The model was also tested on other  $\text{CO}_2$  + polymer systems with varying strengths of interactions and polymer free volumes. While both specific interactions and a higher polymer free volume contribute to increased plasticization of a polymer by  $\text{CO}_2$ , our results appear to indicate that the effect of specific interactions dominates in associating systems.

## Acknowledgment

This paper is dedicated to Professor Stanley I. Sandler on the occasion of his 70th birthday. Professor Sandler has provided wise counsel and been a personal friend to one of the authors (A.T.) since the days of the author's sabbatical at the University of Delaware more than 30 years ago.

## Literature Cited

- (1) Cooper, A. I. Polymer synthesis and processing using supercritical carbon dioxide. *J. Mater. Chem.* **2000**, *10*, 207.
- (2) Tomasko, D. L.; Li, H.; Liu, D.; Han, X.; Wingert, M. J.; Lee, J.; Koelling, K. W. A review of  $\text{CO}_2$  applications in the processing of polymers. *Ind. Eng. Chem. Res.* **2003**, *42*, 6431.
- (3) Woods, H. M.; Silva, M. M.; Nouvel, C.; Shakesheff, K. M.; Howdle, S. M. Materials processing in supercritical carbon dioxide: surfactants, polymers and biomaterials. *J. Mater. Chem.* **2004**, *14*, 1663.
- (4) Hile, D. D.; Amirpour, M. L.; Akgerman, A.; Pishko, M. V. Active growth factor delivery from poly(D,L-lactide-co-glycolide) foams prepared in supercritical  $\text{CO}_2$ . *J. Controlled Release* **2000**, *66*, 177.
- (5) Hyatt, J. A. Liquid and supercritical carbon dioxide as organic solvents. *J. Org. Chem.* **1984**, *49*, 5097.
- (6) Hildebrand, J. H.; Prausnitz, J. M.; Scott, R. L. *Regular and Related Solutions*; Van Nostrand Reinhold Co.: New York, 1970.
- (7) Dobrowolski, J. C.; Jamroz, M. H. Infrared evidence for carbon dioxide electron donor–acceptor complexes. *J. Mol. Struct.* **1992**, *27*, 211.
- (8) Reilly, J. T.; Bokis, C. P.; Donohue, M. D. An experimental investigation of Lewis acid–base interactions of liquid carbon dioxide using Fourier transform infrared (FTIR) spectroscopy. *Int. J. Thermophys.* **1995**, *16*, 599.
- (9) Shieh, Y.; Liu, K.-H. Solubility of  $\text{CO}_2$  in glassy PMMA and PS over a wide pressure range: The effect of carbonyl groups. *J. Polym. Res.* **2002**, *9*, 107.
- (10) Kazarian, S. G.; Vincent, M. F.; Bright, F. V.; Liotta, C. L.; Eckert, C. A. Specific intermolecular interaction of carbon dioxide with polymers. *J. Am. Chem. Soc.* **1996**, *118*, 1729.



- (11) Ozkan, I.; Teja, A. S. Phase equilibria in systems with specific CO<sub>2</sub>-polymer interactions. *Fluid Phase Equilib.* **2005**, 228–229, 487.
- (12) Kasturirangan, A.; Grant, C.; Teja, A. S. Compressible lattice model for CO<sub>2</sub> + polymer systems. *Ind. Eng. Chem. Res.* **2008**, 47, 645.
- (13) Patel, N. C.; Teja, A. S. A New Cubic Equation of State for Fluids and Fluid Mixtures. *Chem. Eng. Sci.* **1982**, 37, 463.
- (14) Sato, Y.; Hashiguchi, H.; Takishima, S.; Masuoka, H. Prediction of PVT Properties of Polymer Melts with a New Group-Contribution Equation of State. *Fluid Phase Equilib.* **1998**, 144, 427.
- (15) Gibbs, J. H.; DiMarzio, E. A. Nature of the glass transition and the glassy state. *J. Chem. Phys.* **1958**, 28, 373.
- (16) Gibbs, J. H. Nature of the glass transition in polymers. *J. Chem. Phys.* **1956**, 25, 185.
- (17) Wissinger, R. G.; Paulaitis, M. E. Glass transitions in polymer/CO<sub>2</sub> mixtures at elevated pressures. *J. Polym. Sci., Part B: Polym. Phys.* **1991**, 29, 631.
- (18) Wissinger, R. G. Ph.D. Thesis, University of Delaware, Newark, DE, 1988.
- (19) Handa, Y. P.; Kruus, P.; O'Neill, M. High-pressure calorimetric study of plasticization of poly(methyl methacrylate) by methane, ethylene, and carbon dioxide. *J. Polym. Sci., Part B: Polym. Phys.* **1996**, 34, 2635.
- (20) Kikic, I.; Vecchione, F.; Alessi, P.; Cortesi, A.; Eva, F.; Elvassore, N. Polymer plasticization using supercritical carbon dioxide: experiment and modeling. *Ind. Eng. Chem. Res.* **2003**, 42, 3022.
- (21) Condo, P. D.; Sanchez, I. C.; Panayiotou, C. G.; Johnston, K. P. Glass transition behavior including retrograde vitrification of polymers with compressed fluid diluents. *Macromolecules* **1992**, 25, 6119.
- (22) Kiszka, M. B.; Meilchen, M. A.; McHugh, M. A. Modeling high-pressure gas-polymer mixtures using the Sanchez-Lacombe equation of state. *J. Appl. Polym. Sci.* **1988**, 36, 583.
- (23) Arce, P.; Azner, M. Modeling the Thermodynamic Behavior of Poly(lactide-co-glycolide) + Supercritical Fluid Mixtures with Equations of State. *Fluid Phase Equilib.* **2006**, 244, 16.
- (24) Zhang, Z.; Handa, Y. P. An in situ study of plasticization of polymers by high-pressure gases. *J. Polym. Sci., Part B: Polym. Phys.* **1998**, 36, 977.
- (25) Sato, Y.; Yurugi, M.; Fujiwara, K.; Takishima, S.; Masuoka, H. Solubilities of carbon dioxide and nitrogen in polystyrene under high temperature and pressure. *Fluid Phase Equilib.* **1996**, 125, 129.
- (26) Kamiya, Y.; Mizoguchi, K.; Naito, Y. A dielectric relaxation study of plasticization of poly(ethyl methacrylate) by carbon dioxide. *J. Polym. Sci., Part B: Polym. Phys.* **1990**, 28, 1955.
- (27) Condo, P. D. In situ measurement of the glass transition temperature of polymers with compressed fluid diluents. *J. Polym. Sci., Part B: Polym. Phys.* **1994**, 32, 523.
- (28) Conway, S. E.; Byun, H.-S.; McHugh, M. A.; Wang, J. D.; Mandel, F. S. Poly(lactide-co-glycolide) solution behavior in supercritical CO<sub>2</sub>, CHF<sub>3</sub>, and CHClF<sub>2</sub>. *J. Appl. Polym. Sci.* **2001**, 80, 1155.

Received for review March 3, 2010

Revised manuscript received July 22, 2010

Accepted July 23, 2010

IE100479Z